MIC TECHNIQUES IN THE DESIGN OF EXTREMELY BROADBAND REFLECTOMETERS

By

S. Hopfer, S. A. Rinkel, and M. Balfour
General Microwave Corporation
Farmingdale, N. Y.

SUMMARY

The application of MIC techniques to the construction of junction type reflectometers and the extension of the junction concept to include slightly lossy junctions makes it possible to design such devices to cover the extreme frequency range of 2 MHz to 18 GHz with equivalent directivities in excess of 40 dB through X band and in excess of 30 dB through 18 GHz.

The currents at a lossless junction formed by three branches are simply related to the reflection coefficient of a load terminating one of the ports, if the second is terminated by a matched load and the third is used to power the junction. Instruments built on this principle have been designed for the low frequency range. At higher frequencies, the size of the junction, in conjunction with the conventional methods of coupling to the branch currents, presents major difficulties. Accordingly, it will be shown that these difficulties are largely eliminated by the use of MIC techniques and by a generalization of the junction concept to include resistive junctions as well.

Consider the view of a bisected reflectometer showing the interconnections of the outer coaxial portion of the structure and the centrally located film portion. The latter is supported between two parallel ground planes in strip line fashion. For purpose of analysis, consider the circuit of Fig. 1, in which the values of the circuit elements are referred to the junction and are normalized to Z_0. The respective branch currents are given by

$$i_1 = \frac{e}{(1+R_s)F}\left\{1+K+R_s(1-K)\right\} \tag{1}$$

$$i_2 = \frac{e}{(1+R_s)F}\left\{1-K+R_s(1-K)\right\} \tag{2}$$

$$i_o = \frac{-2e}{(1+R_s)F}\left\{1+R_s(1-K)\right\} \tag{3}$$

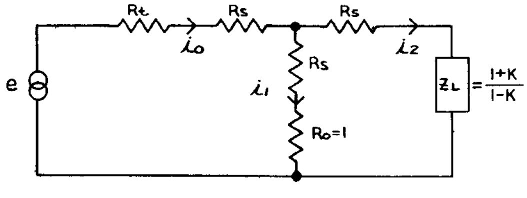

Fig. 1 Circuits Representation at Center of Y Junction - All Component Values are Normalized to Z_0

where K is the reflection coefficient of the load and F is an expression involving R_s, R_t, and K. Accordingly, the ratio of currents as below becomes

$$\frac{|i_1 - i_2|}{|i_o|} = \frac{|K|}{|1+R_s(1-K)|} \tag{4}$$

For the lossless junction $R_s = 0$, the above ratio reduces to $|K|$, and for $R_s \ll 1$, the maximum and minimum values of (4) are given by

$$\max_{\min} \frac{|i_1 - i_2|}{|i_o|} = \frac{|K|}{1+R_s}\left(1 \pm R_s|K|\right) \tag{5}$$

It is seen from (5), that for $R_s \ll 1$, the current ratio determines $|K|$ within a maximum error $\pm R_s|K|$, since the constant factor $(1+R_s)$ can be readily calibrated out by a simple gain adjustment. For example, if $R_s = 0.03$, corresponding to a resistance value of 1.5 Ω in a 50 Ω system, the error is at most 3% for unity reflection coefficient and is entirely negligible for lower VSWR's. Thus, it is seen that a slightly resistive junction, if otherwise desirable, will affect the accuracy in only a minor way. Furthermore, it is evident from (4) and the circuit of Fig. 1, that the ratio of currents is independant of the source impedance R_t and thus does not require the use of a matched generator.

The measurement of the current ratio in accordance with (4) requires that the circuits employed for this purpose respond to the respective currents only and not to the electric fields which exist between the central conductors of the junction and ground. To achieve this condition, one may filter out the electric field components, or balance out the electrically induced effects, or finally, not to couple at all to the electric field. This latter approach, although highly desirable, cannot be realized in a TEM transmission system. However, this objective is partially fulfilled by arranging the detection circuitry coplanar with the inner rf conductors and parallel to the ground planes. In this way, owing to the rapid decrease of the field components as one moves away from the conductors, the major parts of the detection circuitry are located in a field-free region. Moreover, the larger cross sectional dimension in this plane between the inner conductor and ground makes the balancing of electrically induced effects much easier. Evidently, this planar construction is ideal for the application of MIC techniques. In addition, these techniques permit more flexibility in the rf design of the detection circuits and are more amenable to the stringent symmetry requirements of the rf circuits.

Now, it is recognized that by monitoring the rf currents via magnetic induction alone, the detected output would, as far as its frequency response is concerned, have to change as the square of the frequency. This dependance would rule out low frequency operation. Thus, in order to obtain sufficient and essentially constant coupling in the lower frequency range, three current sensing resistances R_s, are introduced in the three branches at the Y junction. The effect of these resistors is to produce voltage drops, proportional to the respective branch currents, and thus to initiate currents in the three detection circuits. By inspection it should be evident that two of the detection circuits separately indicate the quantity $|i_0|$, and that the third detection circuit indicates $|i_1 - i_2|$. The sub-miniature diodes employed are low impedance back diodes, and form an integral part of the detection circuits. If one defines the coupling factor $\mathcal{L}$, as the ratio of the incident power to the Y junction and the power absorbed by the diodes of the first two detection circuits, it can be shown that $\mathcal{L}$ is given by

$$\mathcal{L} = \frac{|3+K|^2}{16} R_d \frac{(1+R_\ell/R_d - \omega^2 L C_d)^2 + \omega^2 (R_\ell C_d + L/R_d)^2}{R_s^2 + \omega^2 M^2} \tag{6}$$

where R_d and C_d are the diode resistance and capacitance respectively; R_ℓ and L are the loop resistance and loop inductance, and where R_s and M are the resistance and mutual inductance of the junction element respectively; K, as before is the reflection coefficient of the unknown load. Inspection of (6) which assumes a matched generator, shows that the coupling factor depends on K, and changes by as much as 6 dB as the load, as seen at the junction, changes from a short circuit to an open circuit. Equation (6) is plotted in Fig. 2, and compared with measured data. The close agreement of the two curves is remarkable, particularly at the high frequencies where the lumped constant circuit approach is not really adequate. The general features of the coupling response are readily identifiable as to their physical significance. Thus, at the very low frequency range, the coupling is constant and governed solely by the resistive parameters of the circuit. As the frequency increases, the induced effects predominate and produce tighter coupling. Eventually, however, the self inductance of the loop and the capacitive shunting of the diode prevent tighter coupling to occur and in fact, reduce the coupling as the frequency is further increased.

It is of interest to determine the limitations in frequency of the three detection circuits. As far as the low frequency limit is concerned, there is in principle no limitation, provided the third detection circuit is perfectly balanced with respect to ground thus eliminating any coupling between the first two detection circuits and the third. As mentioned previously, the MIC techniques employed assure this degree of balance and generally permit equality of resistances within better than 1%, corresponding to equivalent directivities in excess of 40 dB. With respect to the high frequency limitations, there are basically two problems to consider. The first is connected with the difficulty of achieving proper phase balance in the third detection circuit at the higher frequencies. Clearly, if $i_1 = i_2$, then no current should be flowing through the diode of the third detection circuit. At the higher frequencies, this condition will result if the equivalent terminal plane of the diode is positioned in perfect symmetry to i_1 and i_2. Quantitatively, for small phase differences $\theta << 1$, the directivity due to this effect is given by

$$D_{(db)} = 20 \log (\theta/2) \tag{7}$$

For 40 dB directivity this corresponds to path differences of about 0.002 inch at 18 GHz. Fortunately, it is possible to overcome this difficulty by incorporating broad-band phase trimming adjustments, if the corrections to be affected are small to start with. A more severe limitation on the high frequency operation is connected with the fact that relation (4) holds truly only at the center of the junction, yet the currents are monitored slightly away from it. This fact produces an error in the measurement which increases with increasing frequency. An analysis of this effect, with $R_s = 0$, for simplicity, leads to

$$\frac{|i_1(P) - i_2(P)|}{|i_0(P)|} = |K| \times \left| 1 + j \frac{1+K}{2} \tan\beta P \right|^{-1} \tag{8}$$

where P is an equivalent distance from the center of the junction to the point at which the current is effectively monitored, and $\beta = 2\pi/\lambda$. Fig. 3 is a plot of the limits of the indicated values of $|K|$ as given by equation (8) versus $|K|$ itself. Equation (8) has been checked experimentally and found to represent quite adequately the physical situation.

Reflectometers have been built to operate from 2 MHz to 18 GHz with directivities in excess of 40 dB through X band and in excess of 30 dB through 18 GHz.

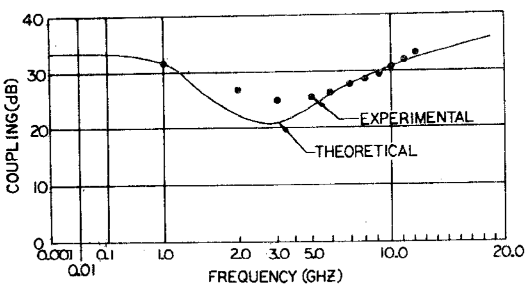

Fig. 2 Frequency Response of Coupling of Detection Circuits

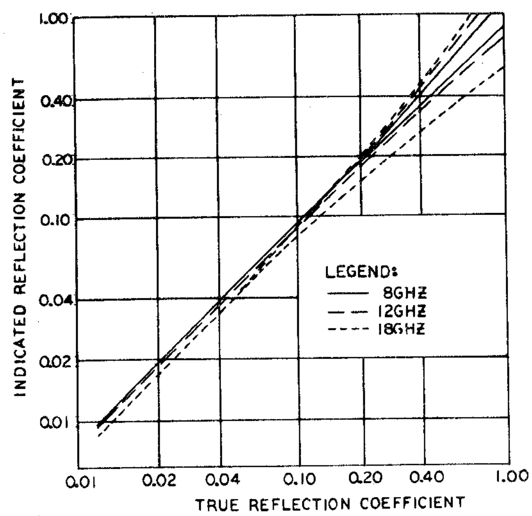

Fig. 3 Limits of Indicated Reflection Coefficient versus True Reflection Coefficient